6596 *Macromolecules* **2009**, *42*, 6596–6605
DOI: 10.1021/ma901237h

Macromolecules
ARTICLE

PLGA−POSS End-Linked Networks with Tailored Degradation and Shape Memory Behavior

Pamela T. Knight,[†,‡] Kyung Min Lee,[†] Taekwoong Chung,[†,‡] and Patrick T. Mather*[,‡,§]

[†]*Department of Macromolecular Science and Engineering, Case Western Reserve University, 2100 Adelbert Road, Cleveland, Ohio 44106,* [‡]*Syracuse Biomaterials Institute and* [§]*Department of Biomedical and Chemical Engineering, Syracuse University, 121 Link Hall, Syracuse, New York 13244*

Received June 9, 2009; Revised Manuscript Received June 25, 2009

ABSTRACT: Biodegradable PLGA oligomers were synthesized to feature a hybrid organic−inorganic moiety, POSS, incorporated at the center of each chain by using it as the ring-opening initiator. After end-capping with vinyl groups, the macromers were photocured into networks with POSS content ranging from 10 to 41 wt %. Increasing POSS inclusion increased the crystallinity of the network while decreasing the degradation rate due to its hydrophobic and nonhydrolyzable properties. It was found that co-curing PLGA oligomers with and without POSS in the backbone could be utilized to create networks with a reduced POSS loading level, at a given cross-link density, allowing tuned crystallinity. Hydrolytic degradation of the co-cured networks was slower than for the PLGA homonetwork but still led to complete degradation after 14 weeks in PBS buffer at 37 °C. The networks exhibited versatile shape memory properties, exploiting the combination of covalent cross-linking and the glass transition, POSS-phase melting temperature, or both as the shape-switching trigger. Using the glass transition was found to yield the best shape fixing, while the best recovery percentages (∼100%) were achieved when the melting transition was used. One network, with 24 wt % POSS, was able to be fixed in a temporary shape by POSS crystallization and to largely preserve this shape during degradation. After 4 weeks and 60% mass loss, 50% of the initial deformation still remained while the PLGA network (shape fixed through T_g) had recovered fully. Our findings are expected to impact future design of biodegradable polymers with shape memory, having revealed the precise tuning of properties possible through controlled placement of a crystallizable and hydrophobic moiety in the polymer network chain.

Downloaded by SYRACUSE UNIV on September 1, 2009 | http://pubs.acs.org
Publication Date (Web): July 22, 2009 | doi: 10.1021/ma901237h

1. Introduction

Rapid growth in the field of polymeric biomaterials has led to remarkable advances in macromolecular design, with even more aggressive goals being set for applicability to the evolving fields of tissue engineering, drug delivery, and implanted medical devices. Consequently, a materials design paradigm emphasizing multifunctionality has emerged, with biocompatibility and/or degradability being supplemented by additional functions, such as a heat-triggered shape change. Polyester-based materials, such as poly(lactide-*co*-glycolide) (PLGA), were once used solely for their controllable biodegradation capabilities but are now being modified, both chemically and physically, in order to meet demanding device requirements. PLGA materials are now not only used as delivery vehicles for drugs and other therapies but also—in manipulated forms—to target cancer,[1] molded into load-bearing geometries such as a screw,[2] to image targeted areas,[3] and can be switched from a temporary shape into a permanent shape through heat or other stimulation.[4,5]

This last property, called shape memory, allows for unique possibilities. For thermally triggered shape memory polymers (SMPs), heat is used to raise the sample above some transition temperature so that the sample is rubbery and deformation can take place. Upon cooling, the sample becomes fixed into a new, temporary geometry. The original shape of the material can then be recovered upon heating once more and under the action of polymer network (either covalent or physical) elasticity. This material property is useful when a complex geometry is desired but is too difficult or expensive to be accomplished during the initial manufacturing process. Postmanufacturing manipulation also allows for customization of the device to meet individual requirements. In order to recover the initial shape after deformation and fixing, a driving force needs to be present such as physical or chemical cross-link points. Covalently cross-linking amorphous or crystalline telechelic oligomers (herein called macromers) has been shown to be an effective way of creating SMPs that can utilize glass transition,[4] clearing temperature,[6] and/or melting point[7,8] as the deformation/fixing temperature. Specifically, photocuring a network is an attractive option due to its applicability in rapid prototyping and creation of photolithographed constructs,[9] as well as having spatial control over cross-link density by using a graded photomask.[10]

Biodegradable SMPs have recently been explored as an alternative to nondegrading implants in which no material remains in the body after serving its function, with degradation achieved either through hydrolytic or enzymatic break down of constituent bonding. Completely amorphous, degradable polymers can be cross-linked in order to create networks that fix and recover a temporary shape around the glass transition temperature, as was shown initially shown by Alteheld et al.[11] Alternately, if the chains are semicrystalline, linear polymers can exhibit T_g-based shape memory using the crystalline physical cross-links as anchoring points to bring the material back to its original form. This has been shown for various copolyesters[12,13] as well as lactide-based polymers with inorganic nanofillers physically mixed in[14] or chemically attached along the backbone.[15] Naturally derived polymers have also been shown to exhibit shape memory properties such as poly(3-hydroxyalkanoates)s. When copolymerized with 3-hydroxyvalerate by the microorganism *Pseudomonas* sp. HJ-2, a semicrystalline film of the material can be stretched and

*Corresponding author. E-mail: ptmather@syr.edu.

 Published on Web 07/22/2009 © 2009 American Chemical Society

Scheme 1. Synthetic Method for the Preparation of POSS-Initiated Poly(DL-lactide-*co*-glycolide)diol, Macromer, and UV Cross-Linked Network

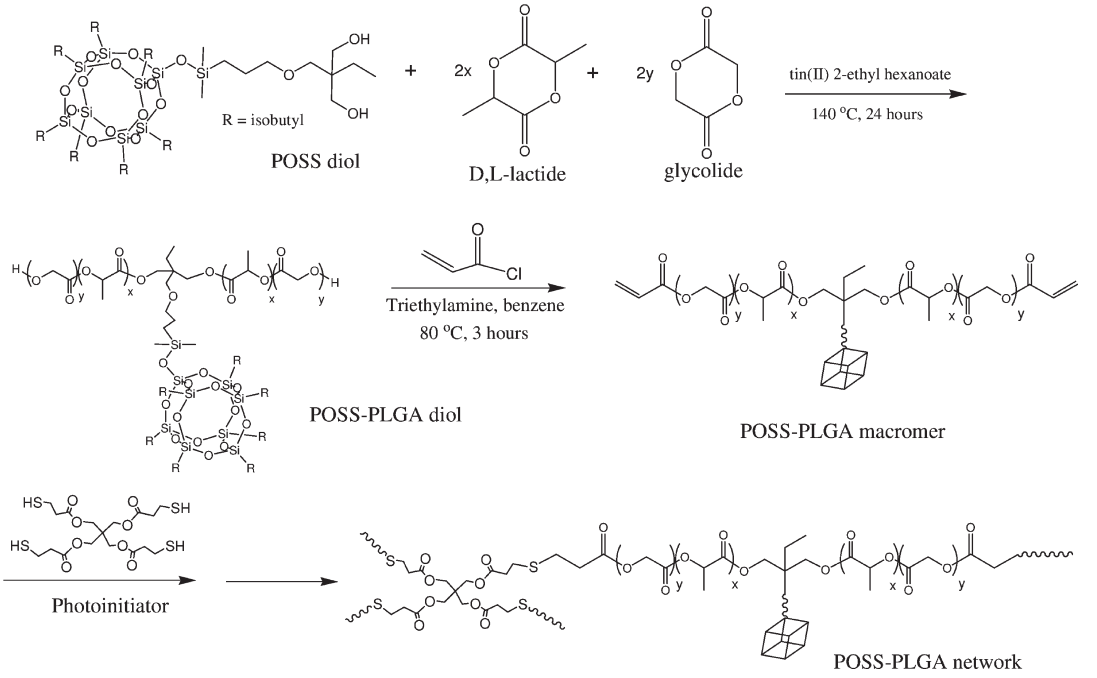

Downloaded by SYRACUSE UNIV on September 1, 2009 | http://pubs.acs.org
Publication Date (Web): July 22, 2009 | doi: 10.1021/ma901237h

fixed at room temperature through the creation of newly ordered domains.[16] The original shape was then recovered by moderate heating.

Recently, our group reported on photocured polycaprolactone-based shape memory networks which incorporated polyhedral oligosilsesquioxane (POSS) along the backbone in order to create physical/chemical double networks.[7] In the present study, PLGA is used as the photocurable macromer and POSS, present in the middle of the macromer backbone, is the only crystallizable segment. This allows for either T_g (which is moderate for a 50:50 lactide:glycolide copolymer) or T_m to be used as the SM transition temperature. Unlike the POSS-PCL networks, inclusion of POSS into the PLGA backbone greatly changes the hydrophilicity of the network and therefore can affect its water uptake and degradation behavior. Since the POSS segments are not hydrolytically degradable at physiological pH, the use of POSS crystallization to fix a shape offers a unique way to maintain a temporary shape, even as degradation occurs.

2. Experimental Section

2.1. Materials. 3,6-Dimethyl-1,4-dioxane-2,5-dione (lactide monomer, LA) was purchased from Aldrich, and 1,4-dioxane-2,5-dione (glycolide monomer, GA) was purchased from Maybridge. Both monomers were purified by recrystallization in ethyl acetate (40 g/200 mL) to give white, flaky crystals. 2-Ethyl-2-[3-[[(heptaisobutylpentacyclo-[9.5.1.1^{3,9}.1^{5,15}.1^{7,13}]octasiloxanyl)oxy]dimethylsilyl]-propoxy]methyl]-1,3-propanediol (or "TMP diolisobutyl-POSS"), hereafter referred to as POSS diol, was purchased from Hybrid Plastics as a pure (>99%) crystalline solid and used as received. Diethylene glycol was purchased from Fluka in ≥99% purity and used without further purification. Tin(II) 2-ethylhexanoate catalyst (Aldrich) was used as received but stored under nitrogen. Benzene (anhydrous), triethylamine, acryloyl chloride, 2,2-dimethoxy-2-phenylacetophenone, and pentaerythritol tetrakis(3-mercaptopropionate) (hereafter, "tetrathiol") were purchased from Aldrich and used as received. All other solvents were purchased from Fisher Scientific and used without further purification.

2.2. Synthesis of POSS-PLGA Telechelic Diol. We followed methods outlined elsewhere for ring-opening polymerizations[17,18] but applied it to our unique composition and architecture. For example, to synthesize a POSS-initated poly(lactide-*co*-glycolide) diol with number-average molecular weight of 4 kg/mol (called P-PLGA4), 2.5 g (17.4 mmol) of recrystallized lactide, 2.0 g (17.4 mmol) of recrystallized glycolide, 1.6 g (1.52 mmol) of dried POSS diol, and ca. 15 mg of tin(II) 2-ethylhexanoate as catalyst were charged into a 50 mL flask under a nitrogen atmosphere. The mixture was stirred continuously at 140 °C for 24 h before cooling to room temperature and dissolving the solid in THF. The solution was precipitated into *n*-hexanes, filtered, and vacuum-dried. Several POSS-initiated PLGA telechelics of varying molecular weights were synthesized, as illustrated in Scheme 1. The amount of POSS used in each synthesis increased as the total molecular weight of the polyol decreased; exact amounts were 5.0 g (4.75 mmol), 2.4 g (2.31 mmol), and 1.6 g (1.53 mmol) of POSS diol for total telechelic molecular weights of 2, 3, and 4 kg/mol, respectively. The synthetic yield for these reactions was typically over 95%. The samples are named using the convention P-PLGA*n*, where *n* indicates the total number-average molecular weight of the diol (in kg/mol) as prescribed by the feed molar ratio of POSS initiator to the cyclic ester monomers and measured using ^{1}H NMR. Gel permeation chromatography (GPC) was also utilized in order to determine the polydispersity of each sample. ^{1}H NMR of P-PLGA4 ($CDCl_3$): 0.106 (s, 6H, $-Si-(CH_3)_2$), 0.595 (q, 16H, $-Si-CH_2-CH-$ and $-Si(CH_3)_2-CH_2-$), 0.945 (q, 45H, $-CH-(CH_3)_2$ and $-C-CH_2-CH_3$), 1.59 (m, 107H, $-CH_2-CH_2-O-$ and $-OOC-CH(CH_3)-O$), 1.86 (m, 9H, $-CH-(CH_3)_2$ and $-C-CH_2-CH_3$), 4.82 (s, 56H, $-OOC-CH_2-O$), 5.24 (m, 35H, $-OOC-CH(CH_3)-O-$).

2.3. Synthesis of DEG−PLGA Telechelic Diol. As a non-POSS control, a PLGA telechelic diol was prepared by initiating the ring-opening polymerization with diethylene glycol (DEG) to form a polyol with a total number-average molecular weight of 4 kg/mol (called PLGA4). To achieve this, 2.5 g (17.4 mmol) of recrystallized lactide, 2.0 g (17.4 mmol) of recrystallized glycolide, 0.12 g (1.16 mmol, $\rho = 1.118$ g/mL) of diethylene glycol, and ca. 15 mg of tin(II) 2-ethylhexanoate as catalyst were charged into a 50 mL flask under a nitrogen atmosphere. The mixture was stirred continuously at 140 °C for 24 h before cooling to room temperature and dissolving the solid in THF. The solution was precipitated into *n*-hexanes, filtered, and vacuum-dried. Gel permeation chromatography (GPC) was

Downloaded by SYRACUSE UNIV on September 1, 2009 | http://pubs.acs.org
Publication Date (Web): July 22, 2009 | doi: 10.1021/ma901237h

utilized in order to determine the final molecular weight and polydispersity of the sample.

2.4. Synthesis of POSS- and DEG-Initiated PLGA Macromers. Each of the synthesized diols described above were end-capped to yield acrylated end groups. For this purpose, 1 mmol of each PLGA telechelic diol (initiated by POSS or DEG) was added to anhydrous benzene under a nitrogen atmosphere along with 2.3 mmol of triethylamine. While stirring, 2.3 mmol of acryloyl chloride was added very slowly to the solution. The reaction was then carried out at 80 °C for 3 h, filtered to remove the resulting triethylamine hydrochloride, and then precipitated in *n*-hexanes and dried under vacuum. The percent yield from the collected product averaged 85%. The extent of acrylate end-capping was determined by NMR and found to range from 90 to 95%. Samples thus converted to the acrylated form are referred to as P-PLGA*n*-mac and PLGA*n*-mac for the samples initiated by POSS and DEG, respectively. ^{1}H NMR of P-PLGA4-mac ($CDCl_3$): 0.106 (s, 6H, $-Si-(CH_3)_2$), 0.595 (q, 16H, $-Si-CH_2-CH-$ and $-Si(CH_3)_2-CH_2-$), 0.945 (q, 45H, $-CH-(CH_3)_2$ and $-C-CH_2-CH_3$), 1.59 (m, 107H, $-CH_2-CH_2-O-$ and $-OOC-CH(CH_3)-O$), 1.86 (m, 9H, $-CH-(CH_3)_2$ and $-C-CH_2-CH_3$), 4.82 (s, 56H, $-OOC-CH_2-O$), 5.24 (m, 35H, $-OOC-CH-(CH_3)-O-$), 5.93 (dd, 1H, $-COO-CH=CH1trans$), 6.19 (dd, 1H, $-COO-CH=CH2cis$), 6.50 (dd, 1H, $-COO-CH=CH_2$).

2.5. Curing of PLGA Homopolymer Networks. To prepare chemically cross-linked networks, the POSS- or DEG-initiated PLGA macromers were mixed with tetrathiol cross-linker and a photoradical generator and then exposed to intense ultraviolet light. For example, P-PLGA4-net was prepared by first adding 0.5 g (0.117 mmol) of P-PLGA4-mac to a 20 mL scintillation vial and dissolving in 1 mL of dichloromethane. Next, 0.059 mmol of tetrathiol cross-linker (1:1 molar ratio of thiol to double bond functionality) and 2 wt % of photoradical generator (2,2-dimethoxy-2-phenylacetophenone) were added. The clear solution was then irradiated with UV light (1200 μW/cm^2) at a wavelength of 365 nm, with a lamp−sample distance of 5 cm, and at room temperature for 1 h. The network was purified with extraction by submerging it in warm dichloromethane (~40 °C) overnight and drying under vacuum at 50 °C prior to analysis. Gel content values ($m_{extracted}/m_{as\text{-}synth}$) were found to be 90%, on average. Network samples are referred to as P-PLGA*n*-net, for POSS-initiated materials, or PLGA*n*-net, for DEG-initiated materials.

2.6. Curing of a PLGA Copolymer Network. To prepare covalently cross-linked networks with a specific weight percent of POSS incorporated, the POSS- and DEG-initiated PLGA macromers were mixed together in a certain amount along with tetrathiol cross-linker and a photoradical generator and then exposed to intense ultraviolet light. For example, P(10)-PLGA4-net (with 10 wt % POSS inclusion) was prepared by first adding 0.20 g (0.0468 mmol) of P-PLGA4-mac and 0.29 g (0.0702 mmol) of PLGA4-mac to a 20 mL scintillation vial and dissolving in 1 mL of dichloromethane. Next, 0.059 mmol of tetrathiol cross-linker (1:1 molar ratio of thiol to double bond functionality) and 2 wt % of photoradical generator (2,2-dimethoxy-2-phenylacetophenone) were added. The clear solution was then irradiated with UV light in the same manner described above for homopolymer network preparation. The network was purified with extraction by submerging it in warm dichloromethane (~40 °C) overnight and drying under vacuum at 50 °C prior to analysis. Gel content values were found to be 90%, on average. The copolymer network sample is referred to as P(10)-PLGA4-net, where the 10 refers to the prescribed POSS weight percent computed relative to the entire material mass.

2.7. Molecular Characterization. To determine the chemical structure and molecular weight (M_n) of the POSS-PLGA diols, ^{1}H NMR spectroscopy (Varian Inova spectrometer, 600 MHz, 64 scans) was performed at room temperature using deuterated chloroform as the solvent. Gel permeation chromatography (GPC) was conducted in HPLC-grade THF using a Varian Pro Star system with a Viscotek dual detector attachment used for viscosity and light scattering measurements. Solutions were prepared from THF (~5 mg/mL) and passed through a 0.2 μm PTFE filter prior to injection. The GPC was operated at a flow rate of 1 mL/min and featured a series of three columns of cross-linked polystyrene beads. The first two columns were 5 and 30 cm long columns (Polymer Laboratories, Inc.), consecutively, each packed with 3 μm particles designed for separations of polymers with molecular weight less than 25 kg/mol. The third column was a mixed-bed column (Tosoh Bioscience GMHHR-M) 30 cm long and featuring a 5 μm particle size affording separation of higher molecular weight polymers.

2.8. Thermal Analysis. The glass transition temperatures (T_g), melting temperatures (T_m), and latent heats of fusion (ΔH) were determined using differential scanning calorimetry (DSC, TA Instruments Q100 equipped with a refrigerated cooling accessory) under a nitrogen purge. As a reproducible thermal history, all diols, macromers, and networks were heated to 150 °C (to erase any previous thermal history), then cooled to −50 °C at a rate of 10 °C/min, and heated once more to 150 °C using the same rate. For comparison, the POSS diol monomer was subjected to the same thermal cycling. Values reported for T_g, T_m, and ΔH are taken from the second heating traces. For comparison with DMA annealing experiments (discussed below), P-PLGA4-net samples were heated to 150 °C, then cooled at 3 °C/min to 60 °C, and held for 5, 30, 60, or 120 min. The samples were then cooled down to −50 °C and heated back up to 150 °C (both at 10 °C/min) in order to observe any change in the POSS latent heat of melting.

2.9. Dynamic Mechanical Analysis and Shape Memory Characterization. Linear viscoelastic thermomechanical properties of the materials were determined using dynamic mechanical analysis (DMA). A TA Instruments Q800 apparatus was employed in tensile mode with a preload force of 10 mN, an oscillation amplitude of 15 μm (0.2%), static stress/dynamic stress amplitude ratio ("force tracking") of 125%, and an oscillation frequency of 1 Hz. Samples were cut from the cured, extracted networks to feature dimensions of 7 mm (length) × 1.6 mm (width) × 0.8 mm (thickness). After loading each film specimen at room temperature under tensile stress, they were heated up to 150 °C to erase all thermal history and then cooled down to 0 °C at 3 °C/min. Once thermally equilibrated, the samples were heated again to 150 °C at 3 °C/min. The second heating traces were recorded and used to determine modulus values. The development of the tensile modulus for the P-PLGA4-net sample was also investigated by first melting, as described above, then cooling to 60 °C at 3 °C/min, and holding isothermally for 2 h. Resulting tensile storage modulus values were taken after 5, 30, 60, and 120 min. For so-called "one-way" shape memory (1W-SM) characterization, samples (in tension) were equilibrated at 150 °C and then cooled down to a deformation temperature of either 120 °C for T_m-based SM or 60 °C for T_g-based SM. The samples were then elongated to a force of 0.3 N at a rate of 0.05 N/min, cooled at a rate of 3 °C/min to either 60 or 25 °C in order to fix the elongated shape, and unloaded to 0.001 N using the same rate as before. The samples were then recovered by heating 3 °C/min to the original deformation temperature (60 or 120 °C). In order to investigate the effect of annealing on the shape memory fixing of the sample, T_m-based 1W-SM runs were performed with various holding times (5, 30, 60, and 120 min) at the fixing temperature, 60 °C. The percentage of fixing, R_f, was calculated as R_f (%) = $(\varepsilon_u/\varepsilon_l) \times 100$, where ε_u is the strain obtained after releasing the applied load and ε_l is the initial strain before the load was released. The percentage of recovery after heating, R_{r1}, was also calculated as R_{r1} (%) = $((\varepsilon_u - \varepsilon_f)/\varepsilon_l) \times 100$, where ε_f is the final strain after heating under no applied load.

To complement T_g-based shape memory analysis, the sample P-PLGA4-net was also investigated using small-angle X-ray scattering (SAXS). A Rigaku S-Max 3000 apparatus with Cu Kα source (λ = 1.54 Å) was used with 30 min exposures at ambient temperature. The SAXS detector was positioned at a sample-to-detector distance of 15.5 cm, allowing detection of structures with *d*-spacings in the range 39.8 nm < *d* < 197 nm.

2.10. Degradation Analysis. In vitro degradation for each of the PLGA networks was performed by immersing a cut sample (50−60 mg) with typical dimensions of 15 mm (length) × 5 mm (width) × 0.8 mm (thickness) in 20 mL of PBS buffer containing 0.05% Tween-20. The sample in buffer was held at 37 °C while being constantly agitated at 75 rpm. The buffer for each sample was decanted and replaced with fresh buffer every 7 days. At predetermined time points, two samples were retrieved from the buffer, rinsed three times with deionized water, patted dry, and weighed. The samples were then dried for at least 5 days at room temperature under vacuum before being weighed again. The water uptake and mass percent remaining were calculated using the following equations:

$$\text{water uptake } (\%) = \left(\frac{m_w - m_d}{m_d}\right) \times 100 \quad (1)$$

$$\text{mass remaining } (\%) = \left(\frac{m_d}{m_{orig}}\right) \times 100 \quad (2)$$

where m_w is the mass of the wet sample, m_d is the sample after drying under vacuum, and m_{orig} is the mass of the original, nondegraded sample.

In order to test the ability of POSS crystallization to fix a temporary shape while the network undergoes hydrolytic degradation, P-PLGA4-net was manipulated using two different methods described below. A criterion for the temporary shapes was facile characterization by dimensional measurements following in vitro treatment. As such, we adopted a simple folded-bar geometry. Method 2 involved elevated temperature annealing, which necessitated use of a glass spacer to prevent self-adhesion. *Method 1* (*quick cool*): Samples with average dimensions of 13.5 mm (length) × 3.5 mm (width) × 1.0 mm (thick) were heated above 100 °C using a heat gun, then folded in half, and held pinched together until cooled to room temperature. The samples were then placed in the refrigerator (∼8 °C) for 5−10 min for further cooling. Non-POSS network samples were also prepared in this manner in order to compare shape fixing solely based on the glass transition (i.e., no crystallization possible). *Method 2* (*anneal*): Samples with average dimensions of 13.5 mm (length) × 3.5 mm (width) × 1.0 mm (thick) were heated above 100 °C using a heat gun, then folded in half over a glass microscope slide, and held pinched together with a clip between two other microscope slides. The entire ensemble was put in an oven at 60 °C and left there for 2 h. The sample was allowed to cool to room temperature and then placed in the refrigerator (∼8 °C) for 5−10 min for further cooling.

After either method of shape fixing was performed, the folded-bar samples adopted a hairpin shape that relaxed during shape recovery (or incomplete fixing) to a triangular shape (Λ). The fixed samples were weighed, and the distance between the two film ends, defined as L_0, was measured. The samples were then degraded in the same manner as discussed above. Recovery to the initial, rectangular shape transpired as an opening hinge and was recorded by measuring the change in the distance between the two film ends and computing the angle of the bend using the formula

$$\frac{L_t}{2} = b \sin\left(\frac{\theta}{2}\right) \quad (3)$$

Here, L_t is the distance between the two film ends at time t, b is the length of one side of the isosceles triangle, and θ is the angle of the bend in the film. Using eq 3, the initial angles of the bent films were calculated as well as the angle of the bend at each degradation time point. To properly normalize the bend angle data as a measurement of shape recovery (ranging from 0 to 100%), we define the recovery percentage here, R_{r2}, as

$$R_{r2}\ (\%) = \frac{\theta_t - \theta_f}{\theta_i - \theta_f} \times 100 \quad (4)$$

where θ_t is the angle of the bend at time t, θ_f is the initially fixed angle of the sample bend (close to zero), and θ_i is the initial angle of the prebent sample, in all cases 180° (flat).

3. Results and Discussion

3.1. Synthesis and Characterization of POSS- and DEG-Initiated PLGA Telechelics. A series of POSS−PLGA telechelic diols were synthesized with various PLGA lengths using POSS diol as the difunctional initiator to ring-open polymerize a 50:50 mixture of lactide and glycolide monomers in the presence of tin(II) 2-ethylhexanoate as a catalyst. The target molecular weight of the POSS−PLGA telechelics, including initiator (M_n = 2, 3, and 4 kg/mol), was controlled by the molar ratio of cyclic ester monomers to POSS diol, thus placing POSS (M_{POSS} = 1052 g/mol) in the center of two PLGA arms each with a predetermined length. As a control, a non-POSS PLGA diol was also synthesized by initiating a 50:50 mixture of lactide and glycolide with diethylene glycol (DEG) and having a total molecular weight of 4 kg/mol. The actual M_n of the POSS-containing diols was determined by ^{1}H NMR using POSS as the internal standard and adapting a technique previously described.[7] Briefly, the integration of the proton peak for the two methyl groups pendant to the noncage silicon on POSS was chosen to reflect one POSS molecule; i.e., the integral was set to 6. Noting that there is only one POSS molecule per chain; subsequent integration of the proton attached to the chiral center of lactide (5.1 ppm, 1H) gives the degree of polymerization (DP) for the lactide repeat unit. Assuming that a true 50:50 mixture of lactide and glycolide was used and incorporated into the original reaction, the DP determined for the lactyl units is also presumed to be that of the glycolide repeat unit. The molar mass for each component could then be determined by multiplying the DP by half of the monomer molecular weight, since each monomer yields two repeat units. Using this methodology, the total M_n values were then determined by adding the molar masses of the lactide, glycolide, and POSS components. All determined values were within 10% of the target molecular weight, as is shown in Table 1. For the DEG−PLGA diol, no such internal standard was available; therefore, the molecular weight was assumed to be the same as that prescribed from the reaction feed. The weight percentage of POSS present in the POSS-initiated diols ranged from 26 to 48 wt %. GPC experiments revealed smooth, monomodal curves for each of the diols with relativity small polydispersity indices, where M_w/M_n was always less than 1.4.

DSC second heating curves for the POSS- and DEG-initiated PLGA diols are shown in Figure 1 and are compared to the pure POSS diol monomer. Analysis results for the same are summarized in Table 1. The glass transition temperature of the PLGA diol was found to increase from 24 to 34 °C when increasing the total molecular weight of the polyol from 2 to 4 kg/mol. The POSS-initiated PLGA diols showed a second thermal transition in the form of POSS melting. Both the melting temperature and heat of fusion values increased with increasing POSS content (i.e., decreasing total polyol M_n), which is opposite to the trend seen for the glass transition temperature. Surprisingly, the melting temperatures found for the POSS−PLGA diols were all equivalent to or exceeded that of the pure POSS diol

Downloaded by SYRACUSE UNIV on September 1, 2009 | http://pubs.acs.org
Publication Date (Web): July 22, 2009 | doi: 10.1021/ma901237h

Table 1. Molecular Characteristics and DSC Results for POSS−PLGA Diols, Macromers, and Cross-Linked Networks

sample name	M_n (g/mol)	POSS content (wt %)	$T_{g,PLGA}$ (°C)[e]	$T_{m,POSS}$ (°C)[e]	ΔH_{sample} (J/g) [ΔH_{POSS} (J/g)]
P-PLGA2	2200[a]	47.8[a]	24	137.2	9.69 [20.3]
P-PLGA2-mac	2380[c]	45.5[c]	26	126.5	9.32 [20.5]
P-PLGA2-net		41.2[d]	36	106.3	4.32 [10.5]
P-PLGA3	3200[a]	32.9[a]	29	133.0	7.81 [23.7]
P-PLGA3-mac	3380[c]	31.8[c]	31	120.8	6.49 [20.4]
P-PLGA3-net		29.6[d]	37	92.5	2.15 [7.26]
P-PLGA4	4100[a]	25.7[a]	34	126.7	3.39 [13.2]
P-PLGA4-mac	4280[c]	25.0[c]	34	116.8	5.05 [20.2]
P-PLGA4-net		23.6[d]	37	85.2	2.00 [8.47]
PLGA4	4000[b]	0	33		
PLGA4-mac	4110[c]	0	31		
PLGA4-net		0	42		
P(10)-PLGA4-net		10	39		

[a] Determined from ^{1}H NMR. [b] Calculated based on the molar feed ratio. [c] Calculated values based on each acrylate end group having MW = 55 g/mol. [d] Calculated values based on the mole ratio of macromer to cross-linker being 2:1 and the tetrathiol having MW = 489 g/mol. [e] Determined from DSC second heating traces.

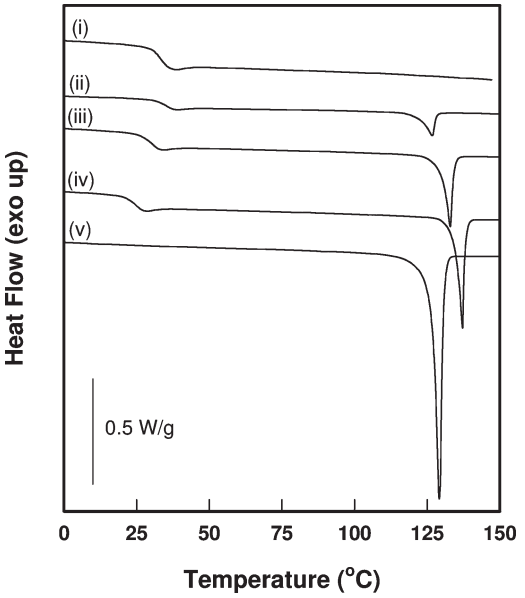

Figure 1. DSC second heating trace of (i) the non-POSS diol, PLGA4, (ii) the POSS-containing P-PLGA4, (iii) P-PLGA3, and (iv) P-PLGA2 diols as well as (v) the POSS diol monomer.

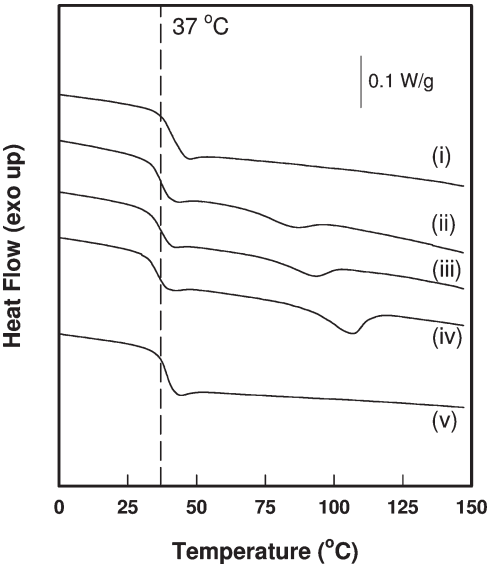

Figure 2. DSC second heating traces for (i) the non-POSS PLGA homopolymer network, PLGA4-net, the POSS−PLGA homopolymer networks: (ii) P-PLGA4-net, (iii) P-PLGA3-net, and (iv) P-PLGA2-net as well as (v) the copolymer network, P(10)-PLGA4-net.

($T_{m,POSS}$ = 130 °C). From the heats of fusion of the polyols (after correcting for the wt % of POSS in each sample) and the heat of fusion for the pure POSS diol (24.75 J/g), the crystallinities of the POSS component in P-PLGA2, P-PLGA3, and P-PLGA4 were calculated to be 82%, 96%, and 53%, respectively. Interestingly, the P-PLGA3 diol was more crystalline than the P-PLGA2, indicating a possible molecular weight limitation to the favorable mixing of POSS and ester repeat units. On the other hand, as the total molecular weight increased to 4 kg/mol, POSS crystallization was hindered by the presence of the longer amorphous polyester chains.

3.2. Synthesis and Characterization of PLGA Homopolymer and Copolymer Networks. The aforementioned telechelic diols were subsequently end-capped with acrylate groups and photocured using a tetrathiol cross-linker in order to create cross-linked, degradable networks. Three different types of networks were explored: (1) one DEG-initiated PLGA network, (2) three POSS-initiated PLGA networks with varying molecular weight between cross-links, and (3) one copolymer network containing 10 wt % POSS through the cocuring of POSS- and DEG-initiated PLGA macromers. Second heating traces for each of the networks are shown in Figure 2 with the analyzed properties being listed in Table 1. For each of the POSS-initiated homopolymer networks, the glass transition temperature for the polyester component was found to be ~37 °C, regardless of the molecular weight between cross-links. However, the weight percent of POSS included in the network, as prescribed by the DP of tethered ester units, directly affected the crystallinity of the system. Both the POSS melting temperature and the heat of fusion of the network increased with increasing POSS content, although these properties were diminished from those found for the corresponding telechelic diols. Upon dilution of the total weight percent of POSS to 10% by co-curing POSS- and DEG-initiated PLGA, as is the case for the copolymer network P(10)-PLGA4-net, no POSS melting was observed by DSC and the T_g increased to 43 °C. This decrease in chain mobility is thought to come from an enhanced mixing of POSS and polyester segments due to the irregular positioning of the potentially crystalline POSS moieties along the network backbone. For the DEG-initiated PLGA network, PLGA4-net, the glass transition was only a few degrees higher than the POSS-initiated versions at 42 °C.

Downloaded by SYRACUSE UNIV on September 1, 2009 | http://pubs.acs.org
Publication Date (Web): July 22, 2009 | doi: 10.1021/ma901237h

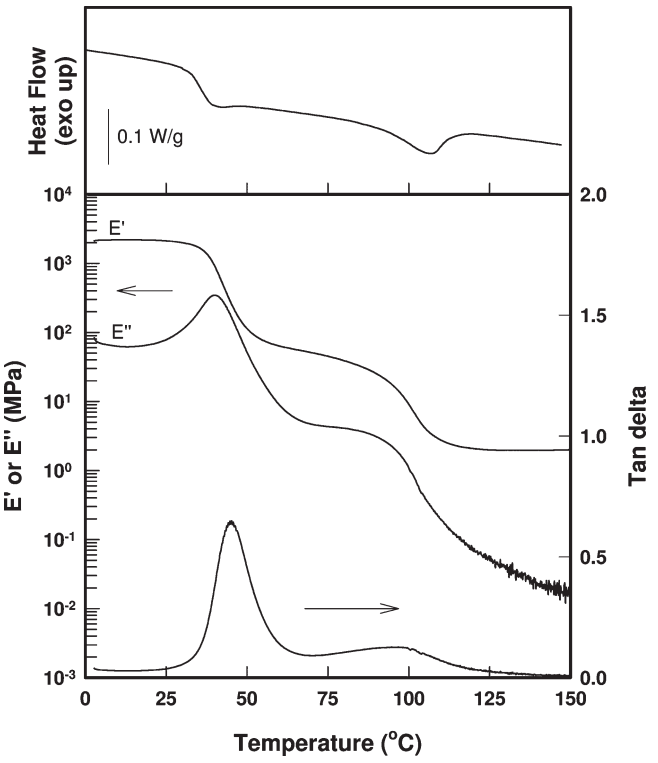

Figure 3. (bottom) Tensile dynamic mechanical analysis (DMA) measurements for P-PLGA2-net, compared with (top) thermal transitions observed by differential scanning calorimetry (DSC).

3.3. Mechanical Properties of the Networks. Inclusion of the POSS moiety into the backbone of PLGA not only affords crystallinity but also increases the tensile modulus both above and below the glass transition temperature. Figure 3 gives the temperature-dependent tensile storage modulus, loss modulus, and tan(δ) data for P-PLGA2-net, the network containing the highest concentration of POSS (41%), along with the associated DSC trace for comparison. This sample shows two thermal transitions: a glass transition from the PLGA covalently cross-linked network and a melting transition from the POSS crystalline regions, resulting in two rubbery plateaus similar to what was observed in a previously reported POSS-PCL double network.[7] At low temperatures ($T < T_g$), the sample was glassy with a tensile storage modulus well above 2 GPa. As the glass transition temperature of the amorphous polyester chains is traversed, the storage modulus drops dramatically to a value below 100 MPa, giving rise to the first rubbery plateau. Upon further heating, the plateau was found to gradually decay, as is typical for most semicrystalline networks approaching the melting point, until near 100 °C (corresponding to POSS crystal melting) where the storage modulus drops again and yields the second rubbery plateau at ~2 MPa.

Each of the POSS-containing homopolymer networks exhibited similar tensile storage modulus versus temperature traces, as shown in Figure 4, with two apparent rubbery plateaus. As POSS content decreases, the initial drop in modulus around 40 °C (T_g of the network) becomes more dramatic, falling to ~20 and ~10 MPa for P-PLGA3-net and P-PLGA4-net, respectively. At temperatures above the POSS melting transition, the final tensile storage moduli of the networks follow a trend consistent with rubber elasticity theory: the modulus decreases as the molecular weight between cross-link junctions increases. Inspection of the results for the copolymer network, trace iv, show that the

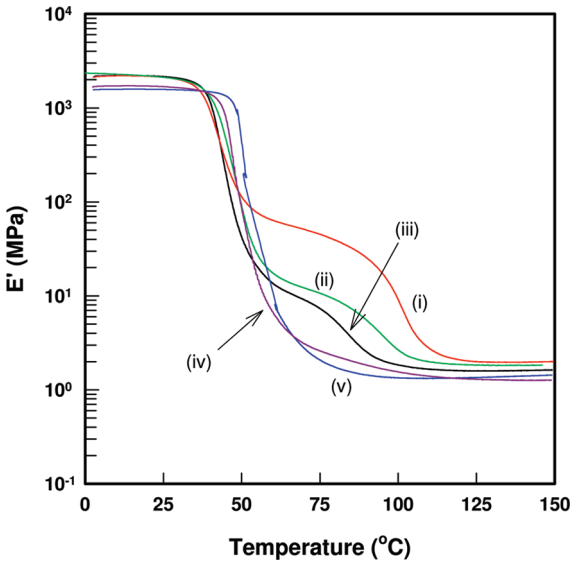

Figure 4. Tensile storage modulus (E') for all POSS-PLGA networks: (i) P-PLGA2-net (red), (ii) P-PLGA3-net (green), and (iii) P-PLGA4-net (black). For comparison, the copolymer network, (iv) P(10)-PLGA4-net (purple), and non-POSS PLGA network, (v) PLGA4-net (blue), are shown as well.

two softening transitions are still observed, although the POSS-based melting is quite diminished. In order to observe the POSS melting transition more clearly, the P(10)-PLGA4-net modulus data along with the corresponding tan(δ) trace can be found in the Supporting Information. In particular, the tan(δ) curve shows two separate peaks with the lower temperature peak indicating a glass transition and the higher temperature transition around 90 °C (a shoulder peak) due to POSS melting. Considering this observation, it can be deduced that some POSS aggregation exists in the copolymer network even though no obvious melting was revealed in the DSC curve. For the non-POSS network, PLGA4-net, the sub-T_g storage modulus trace is much the same as the POSS-containing analogues, although the starting E' value is observably lower at 1.6 GPa and extends out farther due to the slightly higher T_g value. No secondary plateau is observed for this amorphous network, and the modulus quickly drops to ~1 MPa above $T = 80$ °C.

3.4. Shape Memory Behavior of P-PLGA4-net. Utilizing the superambient glass transition temperature of the homopolymer and copolymer networks, one-way shape memory (1W-SM) behavior is possible for any of the aforementioned PLGA networks. When POSS is incorporated, a second method of fixing/recovering an induced deformation is introduced through the crystallization/melting of the POSS moieties. In order to study both the T_g-based and T_m-based 1W-SM properties of these networks, P-PLGA4-net (with 24 wt % POSS) was explored in detail. Figure 5 shows a 1W-SM cycle encompassing both the glass transition and POSS melting and was performed in the following manner. The rectangular sample film was loaded in tension and heated to 150 °C in order to erase all previous thermal history and then cooled down to 120 °C (still above POSS melting). The sample was then elongated (a) by ramping to a stress of 0.34 MPa at 0.06 MPa/min. This temporary shape was fixed (b) by cooling at a rate of 3 °C/min to 25 °C at constant stress, thereby cooling below both the POSS melting temperature and glass transition of the network. The sample was then unloaded (c) to 0.001 N (2 Pa) and triggered to recover the fixed strain (d) by heating to 120 °C at 3 °C/min. From this sequence, a moderate strain of 30% was induced during

Downloaded by SYRACUSE UNIV on September 1, 2009 | http://pubs.acs.org
Publication Date (Web): July 22, 2009 | doi: 10.1021/ma901237h

the initial deformation step, and this increased by 6% while cooling/fixing. Although the strain increase during cooling is on the same scale as was reported for the POSS-PCL materials which exhibited two-way shape memory (2W-SM), the increase was uniformly gradual and showed no abrupt upturn, as would be expected for crystallization-induced elongation,[7,19] and therefore 2W-SM was not explored. Subsequent heating after unloading showed two strain recovery events, as expected: the first being attributed to the lower temperature transition from glassy to a rubbery state and the second from the higher temperature POSS melting. Close inspection of the shape memory cycle reveals that shape fixing is quite good (99.5% of the induced elongation was retained after releasing the applied load), as is shape recovery, with the sample being restored to 99% of its original length after heating. While the observed shape memory properties are quite good for this material, the temperature range required to obtain them is both broad and higher than desirable, especially considering that a smaller temperature span, focused around either the glass transition or POSS crystallization, could be used individually to fix/recover an induced deformation.

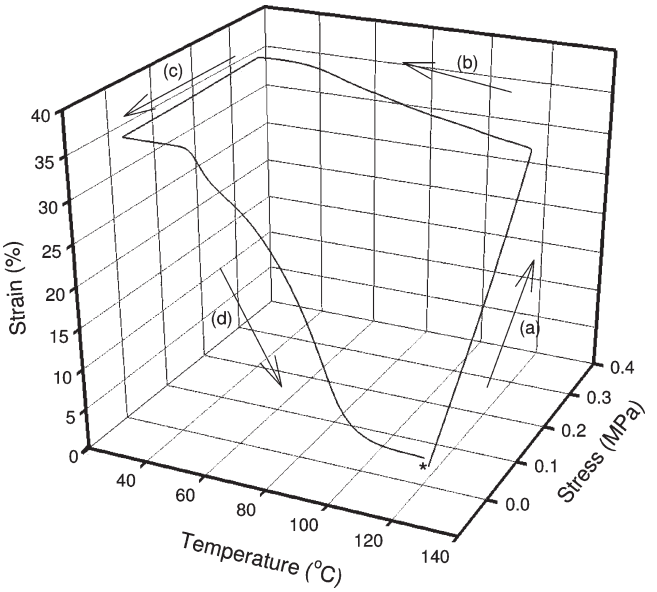

Figure 5. One-way shape memory cycle for P-PLGA4-net with temperatures spanning both the glass transition and POSS melting transitions. The asterisk marks the beginning of the cycle and the arrows denote the various stages, specifically (a) deformation, (b) cooling/fixing, (c) unloading, and (d) recovery.

Since the glass transition temperatures for the PLGA networks are close to that of body temperature (37 °C), T_g-based shape memory was explored. Figure 6a shows three cycles of 1W-SM centered around the glass transition of the material where the sample was deformed/recovered at 60 °C, a temperature found to be between the two rubbery plateaus in the tensile storage modulus trace, and fixing occurred at 25 °C, which is more than 15 °C below T_g. Focusing on the first loop, the sample shows good shape fixing with values of $R_f > 99\%$ (as was seen in Figure 5), but poor recovery with an R_{r1} value of only 27%. On the second and third cycle, ε_l (initial strain before unloading) is *smaller* than the first cycle, dropping from 38% to 36.5% even though the same stress (0.34 MPa) is applied each time. This behavior is opposite that observed for other POSS-based systems for which incomplete recovery was accompanied by proportionally increasing strain from cycle to cycle.[7,15] Interestingly, this sample recovered to almost the same strain of 27.8% for every cycle, irrespective of the initial strain during isothermal deformation. In order to elucidate the origin of the decreasing strain during cycling, T_g-based 1W-SM was also run on the non-POSS homopolymer network, PLGA4-net (Figure S2). The non-POSS analogue was found to have similar fixing capabilities, but a much better recovery of over 90%. The second cycle also *increased* in total strain from the first during the deformation, as is to be expected, and the third cycle was much the same as the second. From this comparison, it was suspected that POSS crystals were the main influencing factor on the decreasing strain during cycling. Small-angle X-ray scattering (SAXS) analysis of P-PLGA4-net confirmed this fact since the POSS crystal domains were found to orient during elongation and retain that orientation throughout recovery at 60 °C (see Supporting Information, Figure S3). Such orientation could also lead to a higher modulus of the material and would account for the decreased total strain observed for the multiple cycles, even though the same applied stress (0.34 MPa) was used every time.

To further elucidate the effect of POSS crystallization on the shape memory properties, 1W cycles were performed

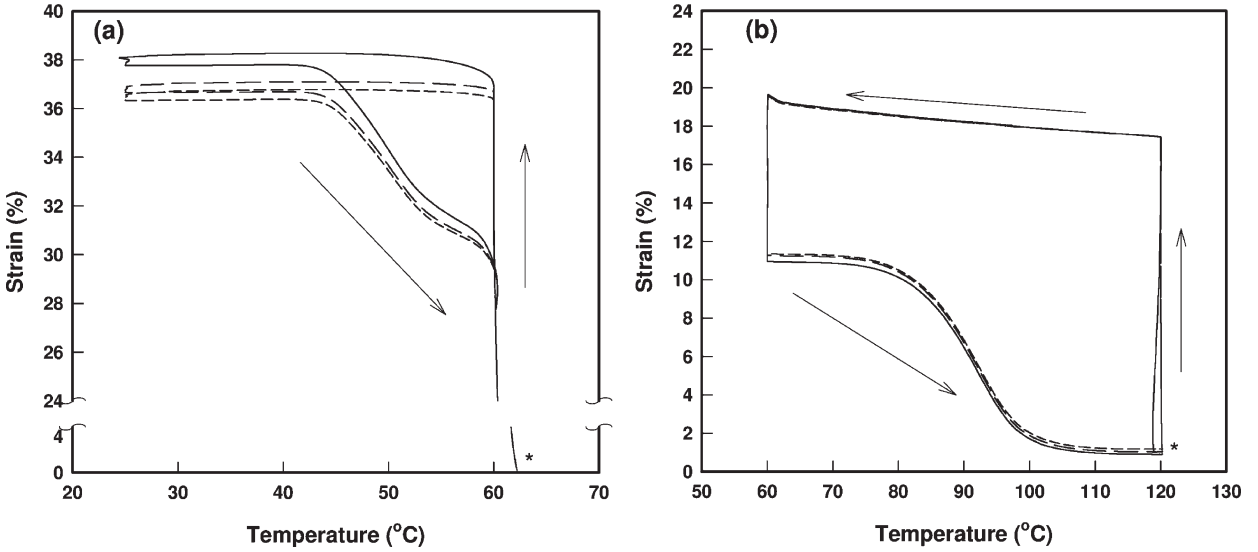

Figure 6. One-way shape memory cycles for P-PLGA4-net based around (a) T_g and (b) T_m. Three cycles are shown: (—) first cycle, (-- --) second cycle, and (- - -) third cycle.

Downloaded by SYRACUSE UNIV on September 1, 2009 | http://pubs.acs.org
Publication Date (Web): July 22, 2009 | doi: 10.1021/ma901237h

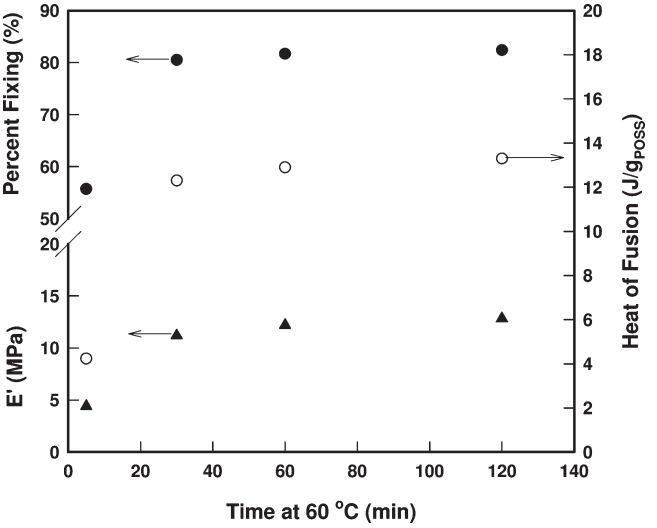

Figure 7. Development of the tensile storage modulus (E', ▲), heat of fusion (ΔH, ○), and T_m-based 1W-SM %fixing (●) for P-PLGA4-net while holding at 60 °C.

around the melting transition. Figure 6b shows the shape memory properties of the P-PLGA4-net material using POSS crystallization/melting as the transition to fix and mediate recovery of an applied elongation. For these T_m-based 1W-SM cycles, the sample was elongated at 120 °C, cooled to 60 °C to fix for 5 min, unloaded, and then heated once more to 120 °C to recover. Each of the three cycles showed very similar results, with poor strain fixing of ~55%, but close to 100% strain recovery. The poor fixing characteristic is thought to result from kinetic limitations. In the prior case of T_g-centered shape memory cycling, the amount of time held at the fixing temperature was inconsequential since the material only had to be equilibrated at a temperature low enough to allow segmental vitrification. When crystallization is utilized, the kinetics of nucleation and growth to the point of mechanical percolation dictate the kinetics of strain fixing. For P-PLGA4-net, annealing a strained sample for 5 min at 60 °C enabled 55% strain fixing. To improve the fixing of the sample, the 1W-SM around T_m was repeated, but the sample was allowed to anneal at 60 °C for 30, 60, and 120 min before releasing the applied force. Figure 7 shows the SM characteristics of the original sample as well as the annealed samples, particularly percent fixing, tensile storage modulus, and total heat of fusion of POSS. As the annealing time was increased from 5 to 120 min, the tensile storage modulus at 60 °C more than tripled (4.4 MPa vs 12.8 MPa) and crystallinity of the sample increased from 17.3% to 53.7% (or 4.24 J/g$_{POSS}$ to 13.3 J/g$_{POSS}$). Most importantly, strain fixing improved with annealing time to a maximum value of 82.4%. The largest jump in all of the aforementioned sample properties was observed within the first 60 min of annealing and increased marginally beyond that time, indicating a maximum beneficial annealing time of 1 h or less.

3.5. In Vitro Degradation of the PLGA Networks. Although PLGA systems are well-known to be bulk degraders in vitro,[20] changes in architecture, composition, and thermal properties can vastly change the degradation behavior. Consequently, we investigated the effect of POSS content on the degradation profile of the PLGA networks by incubating cut samples in PBS buffer at 37 °C over the course of 15 weeks. As shown in Figure 8, the PLGA4-net sample, without POSS present, degraded quickly over the course of 3 weeks and was too fragile to handle at further

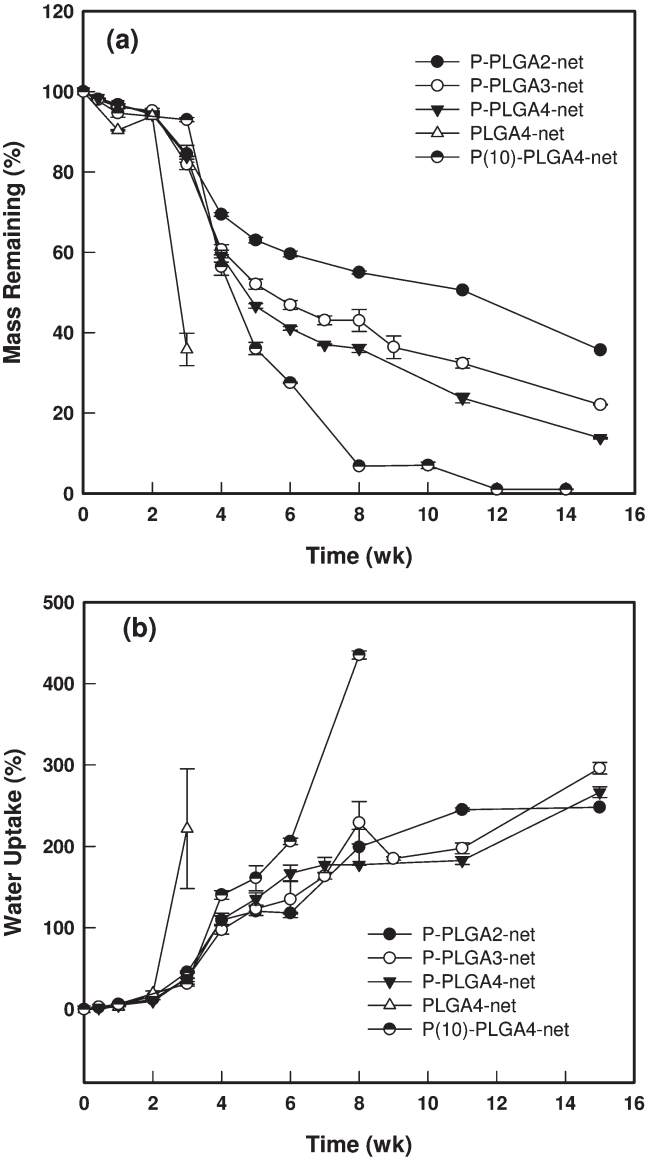

Figure 8. (a) Mass loss and (b) water uptake for the POSS and non-POSS PLGA homopolymer and copolymer networks.

time points. The incubation period for this sample (before significant mass loss began) was found to be about 2 weeks, and complete dissolution was observed in just over 4 weeks. For the POSS-containing networks, the hydrophobic POSS content directly affected how quickly the sample degraded. Samples with the least amount of POSS present degraded the quickest, although the water uptakes observed for all samples, except the non-POSS and copolymer networks, were very similar.

After 15 weeks, each of the POSS-containing networks had remaining mass percentages that corresponded well with their original POSS weight percent, suggesting that POSS itself would take much longer to solubilize than the hydrolyzed ester components. On the other hand, the copolymer network, P(10)-PLGA4-net, dropped below its 10 wt % POSS content during the eighth week of degradation and was completely broken down into soluble units after 14 weeks. We do not yet have a complete understanding of the molecular mechanism behind POSS dissolution into buffer, but we hypothesize that adjacent chain hydrolysis leading to acidic end groups creates POSS-centered amphiphilic molecules that dissolved through micellization. Regardless of the mechanism, the copolymer

Downloaded by SYRACUSE UNIV on September 1, 2009 | http://pubs.acs.org
Publication Date (Web): July 22, 2009 | doi: 10.1021/ma901237h

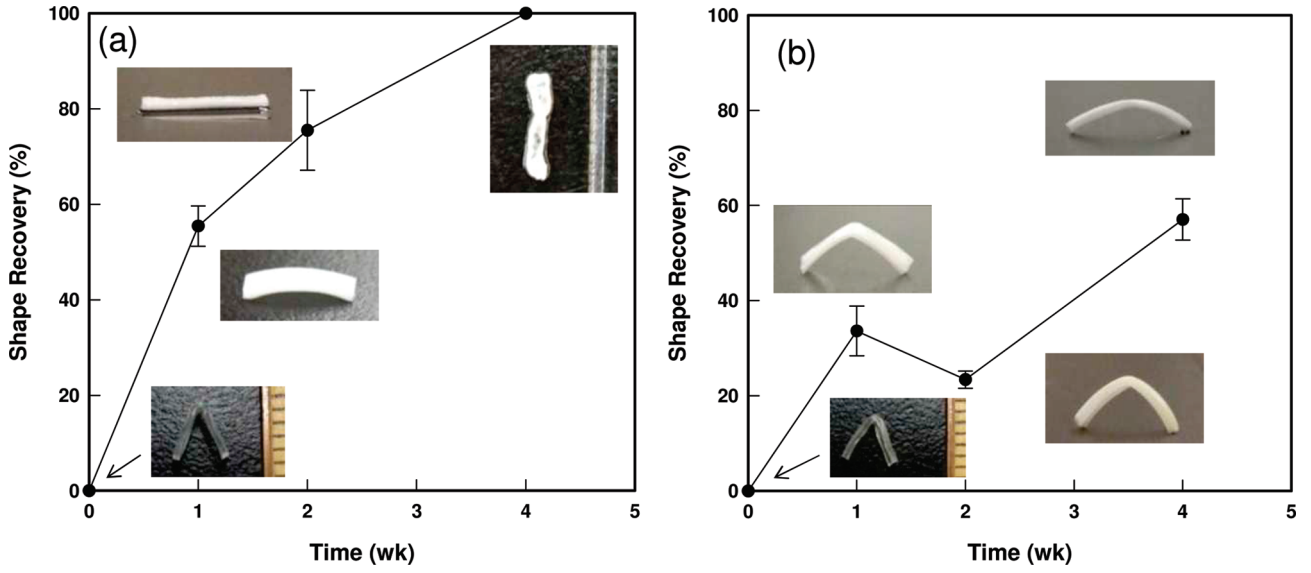

Figure 9. Percent shape recovered for degrading (a) PLGA4-net and (b) P-PLGA4-net while fixed using the *quick fixing* method into a bent, nonequilibrium shape. Representative pictures are given for each time point.

Downloaded by SYRACUSE UNIV on September 1, 2009 | http://pubs.acs.org
Publication Date (Web): July 22, 2009 | doi: 10.1021/ma901237h

network creates a new class of biodegradable material that allows for inclusion of the desirable thermomechanical properties that POSS affords while not hindering complete degradation of the PLGA network.

3.6. Shape Fixing during Degradation of the PLGA Networks. Combining the aforementioned degradation and shape memory aspects of the PLGA-based networks can allow for a wide variety of implantable materials that are able to be manipulated into tailored (e.g., situation-specific) geometries. To create a temporarily fixed shape, the non-POSS PLGA network is capable of being heated and then fixed at room temperature with excellent preservation of the deformed shape, as was seen in Figure S2, until heated above the glass transition temperature which is conveniently situated near body temperature. For applications that require a shape change upon immersion in a physiological environment, such as space filling of an irregular gap, this material is appropriate. On the other hand, after processing the network into a simple film, it may be desirable to fashion the material into a complex geometry that does not recover at 37 °C, even during significant degradation. This type of processing can be accomplished by using the T_m-based, POSS crystallization shape fixing inherent in the POSS-initiated PLGA networks. To explore this feature, degradation of the non-POSS PLGA4-net compared with the P-PLGA4-net material, with a moderate 24 wt % POSS, was observed after fixing each into a "temporary" bent shape. The films were heated to above 100 °C, bent in half, and finally cooled to room temperature under constraint. The samples were further cooled by annealing them at 8 °C for 10 min. After recording the initial angle of the bend, using the distance of the ends and eq 3, these fixed samples were then degraded in PBS buffer in the same manner as above. Figure 9 shows the shape recovery over time for both of the networks as well as representative photographs of the changing shape. The PLGA4-net material (Figure 9a) recovered quickly to a flat piece of film due to the water uptake, effectively lowering the glass transition of the material, as has been reported for polyester systems in aqueous conditions,[21] and allowing recovery to occur. For P-PLGA4-net, the fixed shape lasts much longer and retains ~45% of the original angle even after 4 weeks in vitro. Part of this recovery is most likely due to T_g-based shape fixing since the material was quickly cooled to room temperature and further cooled to a temperature below T_g before POSS crystallization could become extensive. Another factor affecting shape recovery is the swelling of the sample. As seen in Figure 8b, the P-PLGA4-net sample absorbs ~100% of its weight in water after 4 weeks. Swelling of the amorphous regions can cause the crystalline segments to be spread apart and lose their network formation (or "depercolate"), thereby allowing chain relaxation and recovery of the material.

As was seen for the shape fixing discussed above as well as the shape memory properties in Figure 6b, short cooling times are insufficient to allow POSS to crystallize to an extent where good shape fixing is observed. To improve on the aqueous shape fixing, P-PLGA4-net samples were prepared in a similar way as above but allowed to anneal at 60 °C for 2 h before cooling them back down to room temperature. The fate of shape for such samples undergoing degradation can be found in Figure 10. These samples underwent 20% shape recovery over the first 2 weeks (or ~5−10% less than the quick cooled P-PLGA4-net samples). This value corresponds well to the fact that a maximum of 80% shape fixing was observed for annealed samples in Figure 7, and therefore 20% of the fixed shape was expected to recover when the temperature rose above the glass transition. After 4 weeks, the samples had a recovery value, R_{r2}, of ~50%. Like the samples in Figure 9b, it is apparent that once mass loss starts and water uptake increases, the POSS crystal network is disturbed enough that it can no longer hold the temporary shape. Nevertheless, fixed shape retention of the P-PLGA4-net sample far exceeds that of the non-POSS material and may be technologically useful.

4. Conclusions

We have introduced well-defined biodegradable inorganic−organic hybrid network polymers combining PLGA and POSS, with POSS incorporated as a ring-opening polymerization initiator. Both the POSS-centered macromers and end-linked network materials were found to feature crystallization of the POSS moieties within the amorphous PLGA matrix. The polymers were found to feature quite invariant T_g (ca. 37 °C) but variable crystallinity and T_m that each increased with increasing POSS loading. A PLGA/PLGA-POSS conetwork with only 10 wt % POSS incorporation was still found to exhibit POSS

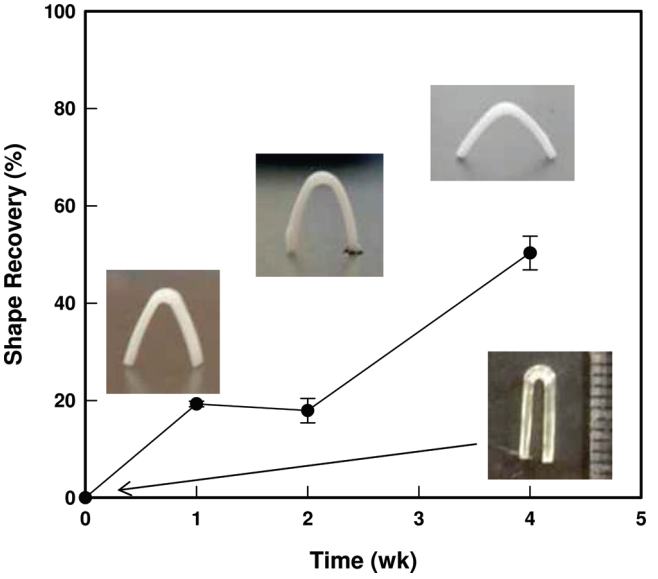

Figure 10. Percent shape recovered for degrading P-PLGA4-net while fixed using the *annealing method* into a bent, nonequilibrium shape. A representative picture is given for each time point.

aggregation and crystallization, but to a much weaker extent. The polymers were biodegradable with a degradation rate that was lowered systematically with increasing POSS content. Shape memory behavior was exhibited by the new materials, with strain fixing possible through POSS-phase crystallization or PLGA-phase vitrification. A sample fixed in a hairpin shape by POSS crystallization largely maintained its shape even to late stages of degradation, while a POSS-free, vitrification-fixed PLGA network recovered completely during degradation, attributed to swelling-induced T_g drop.

Acknowledgment. The authors gratefully acknowledge the support of Boston Scientific Corp. in the form of a graduate fellowship for P.T.K.

Supporting Information Available: (1) Dynamic mechanical analysis and wide-angle X-ray scattering data showing evidence for crystallization of the P(10)-PLGA4-net conetwork; (2) consecutive shape memory cycles around the glass transition temperature of PLGA4-net; (3) small-angle X-ray of P-PLGA4-net during a 1-way shape memory cycle. This material is available free of charge via the Internet at http://pubs.acs.org.

References and Notes

(1) Sun, B.; Ranganathan, B.; Feng, S.-S. *Biomaterials* **2008**, *29*, 475–486.
(2) Ashammakhi, N.; Veiranto, M.; Suokas, E.; Tiainen, J.; Niemela, S.-M.; Tormala, P. *J. Mater. Sci.: Mater. Med.* **2006**, *17*, 1275–1282.
(3) Park, H.; Yang, J.; Seo, S.; Kim, K.; Suh, J.; Kim, D.; Haam, S.; Yoo, K.-H. *Small* **2008**, *4*, 192–196.
(4) Choi, N.-y.; Lendlein, A. *Soft Matter* **2007**, *3*, 901–909.
(5) Kelch, S.; Choi, N.-y.; Wang, Z.; Lendlein, A. *Adv. Eng. Mater.* **2008**, *10*, 494–502.
(6) Rousseau, I. A.; Mather, P. T. *J. Am. Chem. Soc.* **2003**, *125*, 15300–15301.
(7) Lee, K. M.; Knight, P. T.; Chung, T.; Mather, P. T. *Macromolecules* **2008**, *41*, 4730–4738.
(8) Lendlein, A.; Langer, R. *Science* **2002**, *296*, 1673–1676.
(9) Schuster, M.; Infuhr, R.; Turecek, C.; Stampfl, J.; Varga, F.; Liska, R. *Monatsh. Chem.* **2006**, *137*, 843–853.
(10) Wong, J.; Velasco, A.; Rajagopalan, P.; Pham, Q. *Langmuir* **2003**, *19*, 1908–1913.
(11) Alteheld, A.; Feng, Y. K.; Kelch, S.; Lendlein, A. *Angew. Chem., Int. Ed.* **2005**, *44*, 1188–1192.
(12) Lu, X. L.; Cai, W.; Gao, Z. Y.; Tang, W. J. *Polym. Bull.* **2007**, *58*, 381–391.
(13) Zini, E.; Scandola, M. *Biomacromolecules* **2007**, *8*, 3661–3667.
(14) Zhou, S. B.; Zheng, X. T.; Yu, X. J.; Wang, J. X.; Weng, J.; Li, X. H.; Feng, B.; Yin, M. *Chem. Mater.* **2007**, *19*, 247–253.
(15) Knight, P. T.; Lee, K. M.; Qin, H.; Mather, P. T. *Biomacromolecules* **2008**, *9*, 2458–2467.
(16) Kim, Y. B.; Chung, C. W.; Kim, H. W.; Rhee, Y. H. *Macromol. Rapid Commun.* **2005**, *26*, 1070–1074.
(17) Rydholm, A. E.; Bowman, C. N.; Anseth, K. S. *Biomaterials* **2005**, *26*, 4495–4506.
(18) Sawhney, A. S.; Pathak, C. P.; Hubbell, J. A. *Macromolecules* **1993**, *26*, 581–587.
(19) Chung, T.; Romo-Uribe, A.; Mather, P. T. *Macromolecules* **2008**, *41*, 184–192.
(20) Lu, L.; Garcia, C. A.; Mikos, A. G. *J. Biomed. Mater. Res.* **1999**, *46*, 236–244.
(21) Blasi, P.; D'Souza, S. S.; Selmin, F.; DeLuca, P. P. *J. Controlled Release* **2005**, *108*, 1–9.

Downloaded by SYRACUSE UNIV on September 1, 2009 | http://pubs.acs.org
Publication Date (Web): July 22, 2009 | doi: 10.1021/ma901237h